

**Physics of Perturbative Transport  
from Sawtooth Propagation and ECRH Modulation  
in ASDEX Upgrade**

F. Ryter, F. Leuterer, G. Pereverzev, C.J. Fuchs,  
J. Schweinzer W. Suttrop and ASDEX Upgrade Team

*Max-Planck-Institut für Plasmaphysik, EURATOM Association, D-85748 Garching*

### 1. Introduction

The understanding of transport in tokamak plasmas is expected to be improved by comparing results derived from steady-state and transient experiments. This is due to the different physical nature of the transport coefficients deduced in these two cases [1]. In this paper we analyse the electron heat conductivity ( $\chi_e$ ) in ASDEX Upgrade as deduced from power balance ( $\chi_e^{PB}$ ) and from heat pulses ( $\chi_e^{HP}$ ) caused by either sawteeth (ST) or ECRH power modulation. It has been previously shown for this tokamak that sawteeth and ECRH modulation yield different results: the latter yields  $\chi_e^{ECRH}$  values close to power balance ( $\chi_e^{ECRH}/\chi_e^{PB} \leq 2$ ) whereas the former yield  $\chi_e^{ST}$  values without correlation with  $\chi_e^{PB}$  and such that  $1 \leq \chi_e^{ST}/\chi_e^{PB} \leq 6$ , [2]. In this paper we present the  $\chi_e$  profiles deduced from the three methods and discuss possible physical models.

### 2. Experiments

The ECRH system operates at 140 GHz in the second harmonic X-mode. This allows a thin deposition width,  $\leq 5$  cm to compared with  $a = 50$  cm. The absorption is calculated to be 100% in the conditions of the experiments presented here and the supra-thermal population is negligible, the density being above  $4 \cdot 10^{19} m^{-3}$ . We analysed Ohmic and L-mode discharges with different heating powers, plasma currents, magnetic fields and densities, in deuterium and hydrogen. All the discharges were sawtoothing allowing systematic comparison between  $\chi_e^{ECRH}$  and  $\chi_e^{ST}$  [2]. We applied on/off ECRH power modulation with 50% duty cycle with  $P_{ECRH}$  up to 400 kW which is at most half of the heating power. The best results were obtained when the deposition is around mid-radius.

The essential diagnostic for these studies is the 45 channel ECE heterodyne radiometer which provides the electron temperature with a time resolution up to  $\approx 30$  kHz. Generally 30 channels at least were in the interesting plasma region. The radial resolution of each channel is under 1 cm and the distance between channels can be as low as  $\approx 2$  cm. These properties allow to analyse the heat pulse propagation over a large part of the plasma radius and to deduce radial profiles of  $\chi_e^{HP}$ . It must be underlined that a careful independent calibration of the ECE system was performed and that the  $T_e$  measurement is in good agreement with the electron temperature from the Thomson scattering diagnostic. Therefore, both amplitude and phase of the Fourier analysis used below must be considered to have equal weight.

### 3. Analysis

The basis of the data analysis here is a Fourier transformation which yields amplitude and phase of the temperature perturbation for each ECE channel. The calculation of  $\chi_e^{HP}$  follows the method described in [3]. At each radial point of the measurement a  $\chi_e^{HP}$  value is calculated

with corrections for cylindrical geometry and density gradient. The gradient of the temperature perturbation necessary for the calculation of  $\chi_e^{HP}$  is obtained from fit of the data. As usual,

$$\chi_e^{HP} = \sqrt{\chi_e^{Amp} \chi_e^{Phase}}, \chi_e^{Amp} \text{ and } \chi_e^{Phase} \text{ deduced from amplitude and phase.}$$

The time-dependent transport code ASTRA is used to model the steady-state and transient experiments. This code uses the toroidal geometry, the damping (Ohmic power changes and electron-ion exchange) is calculated. The ECRH power modulation is included as a modulated heating term of the electrons with the corresponding frequency and wave form. The deposition is radially defined as a Gaussian with position and width corresponding to the experiment. The ion temperature profile is that of the experiment.

The sawtooth modelling is based on a Kadomtsev reconnection model. The frequency of the sawteeth is prescribed according to the experiment. In our discharges the inversion radius corresponds to the calculated  $q=1$  radius within  $\approx 20\%$ . At each sawtooth crash the  $T_e$  profile is flattened and the energy is redistributed inside the mixing radius. Note that the exact modelling of the sawteeth is not essential in this study, the important part being the creation of a heat pulse outside the mixing radius which will then propagate towards the plasma edge, according to our transport model. The Fourier transformation of the ASTRA results and experimental data are compared to test the validity of different transport models.

#### 4. Results

Examples of results from experiment and modelling are shown in Figs. 1 and 2 for ECRH modulation at 100 Hz and sawteeth respectively, during the same time period of the plasma. This is an L-mode discharge in hydrogen with 2 MW NBI heating, residual Ohmic power of 0.4 MW and line-averaged density of  $5 \cdot 10^{19} m^{-3}$ . The comparison of Figs. 1 and 2 clearly shows that  $\chi_e^{ST}$  is larger than  $\chi_e^{ECRH}$  and that both are larger than  $\chi_e^{PB}$ . Note that is not due to a poor signal to noise ratio for the ST case because the amplitude of the ST perturbation is equal to or larger than that of ECRH and both are above the noise level, indicated in Figs. 1 and 2. It is also underlined that both amplitude and phase yield large  $\chi_e^{ST}$  values. The difference between  $\chi_e^{PB}$  and  $\chi_e^{HP}$  is expected, as already mentioned above [1]. The fact that sawteeth and ECRH yield different values in the same discharge indicates that either the transport mechanism depends on the heat pulse or that two transport mechanisms are acting, depending on the nature of the perturbation. This is investigated in the following.

The first and simplest step in trying to model the transient experiments is to find a time-independent  $\chi_e$  profile which reproduces the transient experimental results. This could be easily achieved for the ECRH modulation for which  $\approx 2 \times \chi_e^{PB}$  gives good agreement with the amplitude and phase profiles of Fig. 1. This is a bench marking between ASTRA and the Fourier analysis and shows that a locally determined diffusive transport may well explain the data. However, this does not include any physics model. For sawteeth it was not possible to find a time-independent  $\chi_e$  yielding good agreement with both phase and amplitude. The disagreement is larger at higher frequency (3<sup>rd</sup> harmonic). This suggests that a non-diffusive transport process is also involved. We tried to reproduce the experimental data from both ECRH and sawteeth with 3 transport models: a local model, a non-local model and a model combining both.

The local model is based on  $\chi_e \sim \nabla T_e^\alpha$ . According to [4] one may conclude from the ratio of about 2 between power balance and ECRH modulation that  $\alpha \approx 1$ . The simulation under this assumption gives rather good agreement for the ECRH case (Fig. 1) but also for the sawtooth case (Fig. 2). However in none of the cases the agreement is perfect. A more precise agreement is obtained for ECRH in Ohmic cases in which the  $\chi_e$  profile is much flatter than in the auxiliary

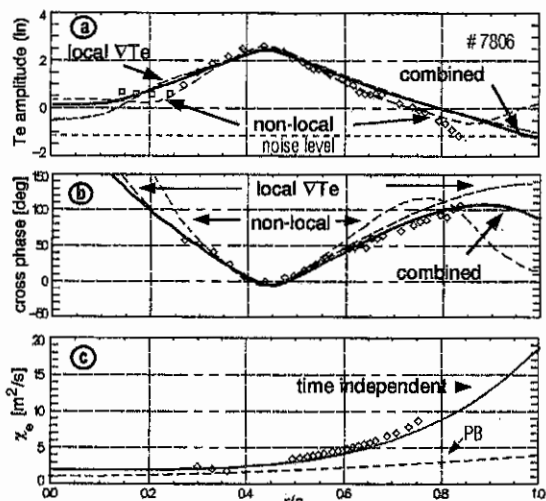


Fig. 1. ECRH modulation: diamonds are experimental data. Dashed lines in a and b are simulations with local and non-local models. The third line is the combination of both local and non-local. The HFS region ( $r/a \leq 0.3$ ) of the amplitude might be perturbed by the sawtooth underground noise.

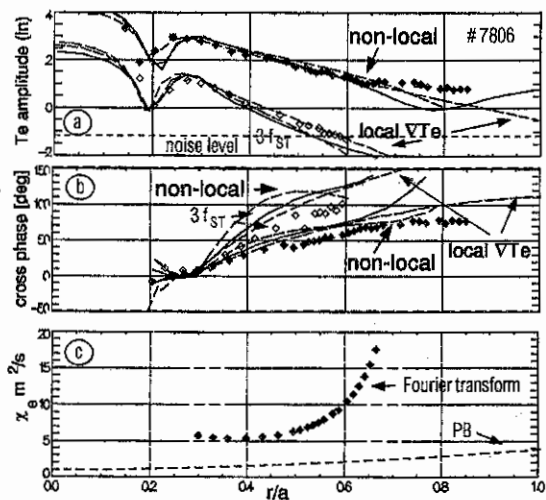


Fig. 2. Sawtooth analysis: Data points are diamonds: closed symbols for fundamental, open symbols for 3rd harmonic. The lines are the three simulation models as in Fig. 1.

heated discharge analysed here [5]. Figures 1 and 2 also show the comparison with our non-local model. Following the non-local power dependence of  $\chi_e$  found for ECRH described in [4], we introduce here for sawteeth the model  $\chi_e(t) = \chi_e^{PB} \times (\bar{T}_{e0}^{ST}(t)/T_{e0})^\beta$ , where  $\bar{T}_{e0}^{ST}(t)$  is the modulation of the central electron temperature caused by sawteeth and  $T_{e0}$  the time-averaged central electron temperature. For ECRH the amplitude of the perturbation is taken at the centre of the ECRH deposition profile. The exponent  $\beta = 1.5$  yields good agreement with the experimental data, as shown in Figs. 1 and 2. Note the precise agreement of the amplitude for the ECRH but the poorer one for the phase. For the sawteeth the agreement for the amplitude is as good as obtained with the local model, but the agreement for the phase is poorer. The two models were combined:  $\chi_e(t) = \chi_e^{PB} \times (\bar{T}_{e0}^{ST}(t)/T_{e0})^\beta \times \nabla T_e$ . The results in Figs. 1 and 2 were obtained with  $\beta = 0.5$ . The simulations are closed to the results from the local model. For ECRH the phase is somewhat better reproduced, for the sawteeth no significant difference appears. Clearly, based on this example non clear statement can be made on the character of the transport in these experiments.

## 5. Discussion and conclusion

The local  $\nabla T_e$  model seems to explain our experimental data but the precision is not excellent. This leaves enough room for large variations in  $\chi_e^{HP}$ , as this quantity depends on the square of the gradients of the phase and amplitude profiles. This is shown by the experimental  $\chi_e^{HP}$  profiles which reach very large values, as shown in Figs. 1 and 2. A non-local model seems to be able, even required to reproduce some features of our data, in particular outside  $r/a = 0.6$ . A non-local model excites an additional  $T_e$  perturbation along the radius where steady-state power exists, [4]. This creates a perturbation standing wave across the plasma. Our non-local model is very simple and uses the temperature change as a switch to vary  $\chi_e$  in time. It clearly has the drawback that  $\chi_e$  is changed instantaneously at the onset of the perturbation. This critically forces the phase of this standing wave to zero at the edge. A more realistic model with a radially dependent delay for reaction of  $\chi_e$  to the perturbation is expected to change this situation. This will be the subject of future work.

## 6. Acknowledgement

It is a pleasure to acknowledge fruitful discussions with A. Jacchia, F. DeLuca, G. Gorini, N.J. Lopes Cardozo, P. Mantica and U. Stroth. We warmly thank P. Mantica for having cross-checked our Fourier analysis and  $\chi_e$  calculation on some ASDEX Upgrade data sets with the methods used for JET and RTP data.

## References

- [1] LOPES-CARDOZO, N. J., *Plasma Phys. Controlled Fusion* **37** (1995) 799.
- [2] RYTER, F. et al., IAEA, Montréal, 1996, F1-CN-64/AP1-5.
- [3] JACCHIA, S. et al., *Phys. Fluids B* **3** (1991) 3033.
- [4] STROTH, U. et al., *Plasma Phys. Controlled Fusion* **38** (1996) 611.
- [5] RYTER, F. et al., *Proceedings EPS 1996, 20C, part I, 11, 1996*.